AIP | Review of Scientific Instruments

Vacuum ultraviolet, extreme ultraviolet, and x-ray line intensity normalization technique applied to tokamak plasmas

N. J. Peacock, K. D. Lawson, R. Barnsley, and H. Chen

Citation: Rev. Sci. Instrum. **70**, 317 (1999); doi: 10.1063/1.1149443
View online: http://dx.doi.org/10.1063/1.1149443
View Table of Contents: http://rsi.aip.org/resource/1/RSINAK/v70/i1
Published by the American Institute of Physics.

Related Articles

Spherical torus equilibria reconstructed by a two-fluid, low-collisionality model
Phys. Plasmas 19, 102512 (2012)

Oblique electron-cyclotron-emission radial and phase detector of rotating magnetic islands applied to alignment and modulation of electron-cyclotron-current-drive for neoclassical tearing mode stabilization
Rev. Sci. Instrum. 83, 103507 (2012)

Toroidal rotation of multiple species of ions in tokamak plasma driven by lower-hybrid-waves
Phys. Plasmas 19, 102505 (2012)

Perpendicular dynamics of runaway electrons in tokamak plasmas
Phys. Plasmas 19, 102504 (2012)

Electron cyclotron current drive modelling with parallel momentum correction for tokamaks and stellarators
Phys. Plasmas 19, 102501 (2012)

Additional information on Rev. Sci. Instrum.

Journal Homepage: http://rsi.aip.org
Journal Information: http://rsi.aip.org/about/about_the_journal
Top downloads: http://rsi.aip.org/features/most_downloaded
Information for Authors: http://rsi.aip.org/authors

ADVERTISEMENT

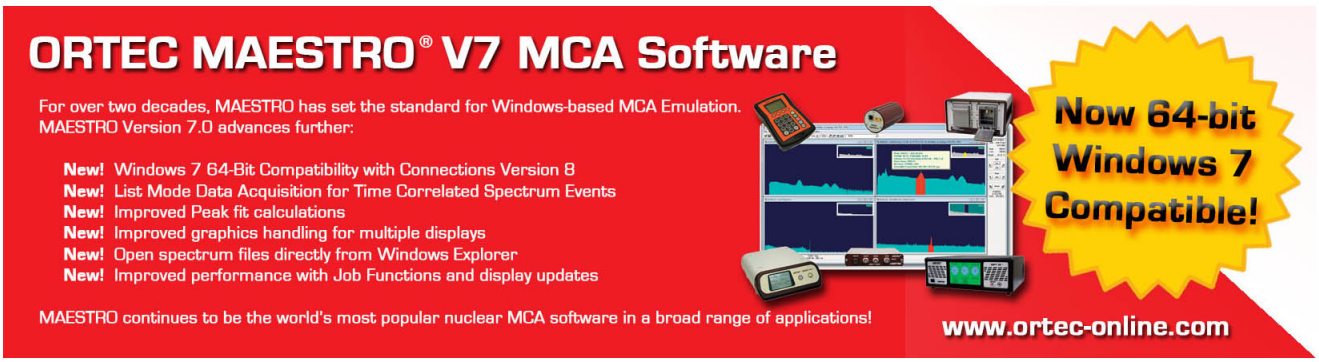

Vacuum ultraviolet, extreme ultraviolet, and x-ray line intensity normalization technique applied to tokamak plasmas

N. J. Peacock and K. D. Lawson
UKAEA-Fusion, Culham Science Centre, Abingdon, Oxfordshire OX14 3DB, United Kingdom

R. Barnsley
JET, Joint European Undertaking, Abingdon, Oxfordshire OX14 3EA, United Kingdom

H. Chen
Blackett Laboratory, Imperial College of Science Technology and Medicine, London, United Kingdom

(Presented on 8 June 1998)

An empirical procedure, ''LINT,'' for relating emission line intensities of intrinsic impurity ions to their elemental contributions to the total, bolometric, radiation loss and the volume-averaged effective ion charge, Z_{eff}, has been developed and applied to limiter plasmas in the JET tokamak. In this article we discuss extensions to the data base to include x-ray lines and continua intensities, applicable to a wider range of tokamak plasma configurations such as *X*-point plasmas and quasi-steady-state, edge-cooled ELMy H modes. Examples are shown of the technique applied to reference discharges during which the plasma configuration is changed continuously. The total data set, comprising line and continua irradiances, tomographic bolometry, and x-ray emission and Z_{eff} imposes constraints on the diffusion parameters used in models of impurity ion transport. © *1999 American Institute of Physics.* [S0034-6748(99)66301-8]

I. INTRODUCTION

A full description of intrinsic and injected impurity ions in a tokamak requires tomographic analyses of the total and the spectrally resolved emission data. Since the availability of tomographic data does not in general span all the emitting species, it is the practice to measure a restricted range of line and continuum radiances and fit these data to an ion transport code such as SANCO[1] which can encompass a relevant atomic data base such as ADAS.[2] Using the population structure code to calculate R_i, the relative excited state population, then the line radiance in terms of the ion abundance q_Z is given by

$$I_{ij}=\frac{\epsilon_{ij}}{4\pi}=n_e q_Z R_i \frac{A_{ij}}{\Sigma A_{ij}} h\nu_{ij}.$$

Given that the local flux of ions of charge state *z*, atomic number *Z*, is described by a diffusive (D) and convective (V) equation

$$\Gamma_Z=-D(r)\nabla n_Z(r)+V(r)n_Z(r),$$

then the concentrations of the ions are given by a solution of the coupled equations

$$\frac{\partial n_Z}{\partial t}=-\nabla.\Gamma_Z+n_e(n_{Z-1}S_{Z-1}-n_Z S_Z+n_{Z+1}\alpha_{Z+1}-n_Z\alpha_Z)$$

$$-\frac{n_Z}{\tau_Z}+\gamma_Z.$$

S and α are the appropriate ionization and recombination coefficients while τ and γ are the loss and influx terms, respectively. Uncertainties in the transport and atomic physics modeling as well as errors in the absolute radiances make these detailed transport simulations a complex, lengthy, and often error-prone procedure.

A novel, empirical method, the line intensity normalization technique (LINT), which is relatively independent of transport, density $n_e(r/a)$ and temperature $T_e(r/a)$ profiles for a set of similar discharges, has been developed on the joint European torus (JET) tokamak to provide routine information on the impurity content of the plasma and elemental components of radiated power (P_{rad}). The LINT method[3] is based upon the hypothesis that a representative ion with a characteristic (VUV) or (XUV) spectral line can be chosen for each significant impurity element within the plasma and that each of these spectral line intensities has a linear relation to the contribution of that element to the total radiated power and to the effective ion charge, Z_{eff}. While being able to quickly process a large number of similar discharges, this empirical approach could be criticized for being both simplistic and lacking in an obvious physical basis. Transport simulations, however, have provided independent evidence[3] of the validity of the technique. Somewhat analogous to the principle of neural networks, the practicality of the LINT method has been demonstrated[3] when applied to a large number of tokamak discharges with a common, e.g., limiter, configuration. Its limitations have been exposed when applied universally to all tokamak plasma configurations. In this article the rationale for the success with one class of plasmas and the shortcomings of LINT with other, especially high confinement regimes, is discussed.

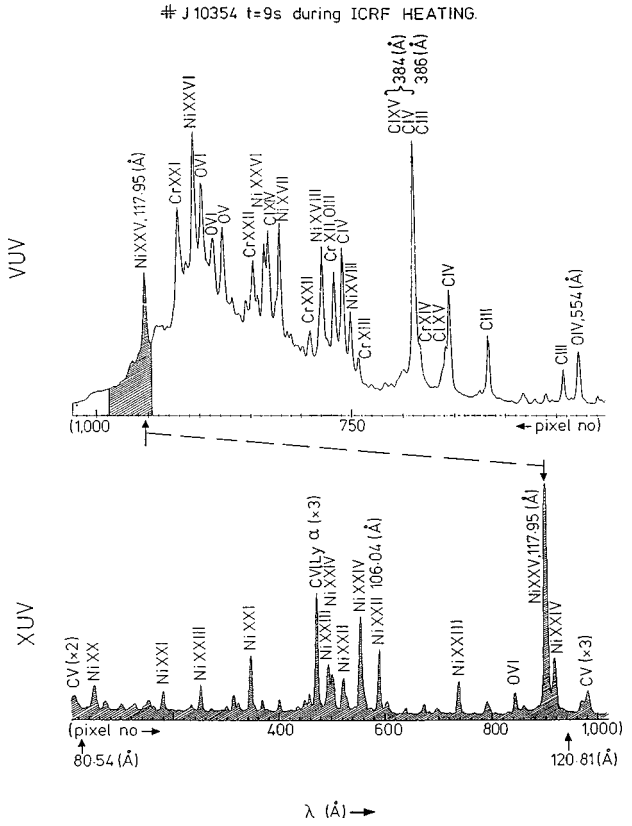

FIG. 1. Sample of VUV (upper) and XUV (lower) line emission from early (No. 10 354) JET plasma with ICRF heating, showing overlap within the 80–120 Å spectral region.

II. ANALYTIC PROCEDURE ASSOCIATED WITH "LINT"

Choice of a specific atomic transition and ion species to represent the elemental contribution to the total radiation is an important aspect of the LINT analysis. From experience, ions located near the edge of in the core plasma are not suitable candidates. Edge ion line intensities are prone to intractable variations due to changes in the edge pressure profile, influxes, and recycling. Core emission is overly sensitive to changes in the peak axial temperature. Ions emitting in the intermediate region, approximately $0.4 \leqslant r/a \leqslant 0.95$, are favored. In practice, this means selecting $\Delta n = 1$ resonance transitions lying in the XUV spectral region for the H-like ions of the light elements, e.g., Be IV, C VI, O VIII and $\Delta n = 0$ transitions for higher Z impurities, these lines, lying in the far VUV spectral region, being relatively insensitive to temperature. Representative ions are Cl XV, Cl XVI, Ar XV, Ar XVI and the neon-shell ions of common metal impurities such as Cr XXI, Fe XXIII, Ni XXV, etc. Demonstration of the LINT analyses has in the past used data from VUV[4,5] and XUV,[6] single line-of-sight spectrometers operating over the range $15\ \text{Å} < \lambda < 500\ \text{Å}$. Samples of the spectral data are illustrated in Fig. 1. Most of the emitting ions illustrated in Fig. 1 lie within the $0.4 \leqslant r/a \leqslant 0.95$ region of the normalized radius. Figure 2 shows the results of a transport model calculation of the distribution of nickel ions for a specific JET discharge (No. 13 738). The 118 Å emission from Ni XXV, for example, is a suitable candidate since, for a set of discharges with self-similar transport and with consistent shapes of $n_e(r/a)$, $T_e(r/a)$, changes in $T_e(r/a=0)$ will cause the ion to move slightly to another location on the $n_e(r/a)$ profile. This does not invalidate the analyses since the ratio of $I_{ij}/P_{\text{RAD}(Z)}$ remains independent of n_e.

In practice the LINT normalization factor $C_{\text{RAD-}Z}$ relating I_{ij} to $P_{\text{RAD-}Z}$ (and $C_{\text{eff-}Z}$ to Z_{eff}) is derived by adjusting the the C scalings until the sum of all the elemental components match the total radiative power measured by bolometry.[7] The quantity $P_{\text{RAD-BOLO}}(t) - \Sigma C_{\text{RAD-}Z} I_{ij}(t)$ is minimized. It is a significant help if during a discharge only one impurity concentration alters at any one time; ideally all other parameters being kept constant. Then there is a clear individual relation between the line intensity and the incremental bolometric measure. In the case of the Z_{eff} components, each spectral line intensity, as well as being scaled linearly, is divided by a measure of n_e^2 so as to represent the impurity concentration. The volume averaged n_e has routinely been used in the JET analysis. The concentrations are then converted to Z_{eff} components and the significant components are summed. The sum is matched to the Z_{eff} as determined from visible bremsstrahlung measurements,[8] by minimizing the quantity:

$$Z_{\text{eff}}(t,[\text{bremss.}]) - 1 - \sum_{Z=1}^{Z(\text{Max})} \frac{C_{\text{eff-}Z} I_{ij}(t,[z])}{\langle n_e 2(t) \rangle^2} \overline{z(z-1)}.$$

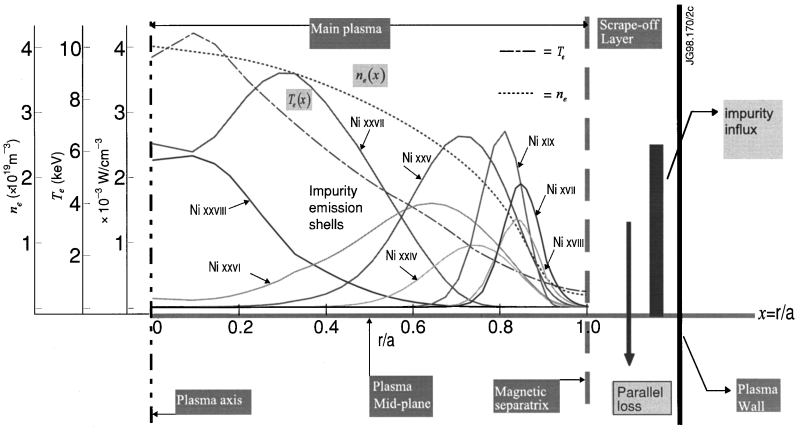

FIG. 2. Distributions of VUV line emissivities from intrinsic Ni ions in JET plasma (No. 13 738), modeled using the diffusive equilibrium code SANCO.

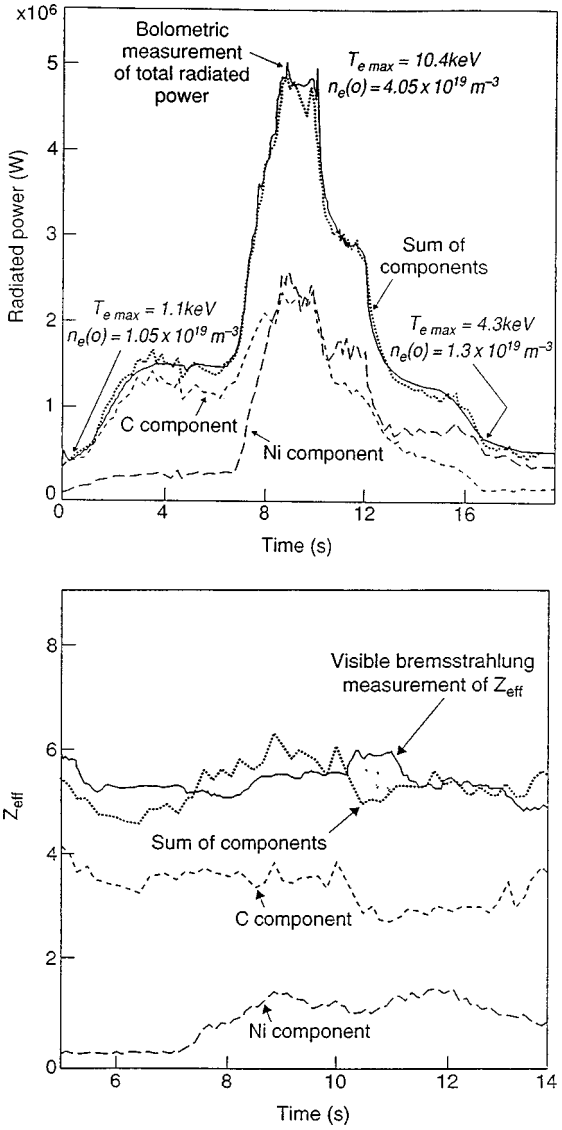

FIG. 3. (upper) Elemental P_{rad} components, the components' sum and the total radiated power and (lower) Z_{eff} measurements and components of Z_{eff} together with their sum for pulse No. 13 728 showing the contributions of the two dominant impurities, C and Ni.

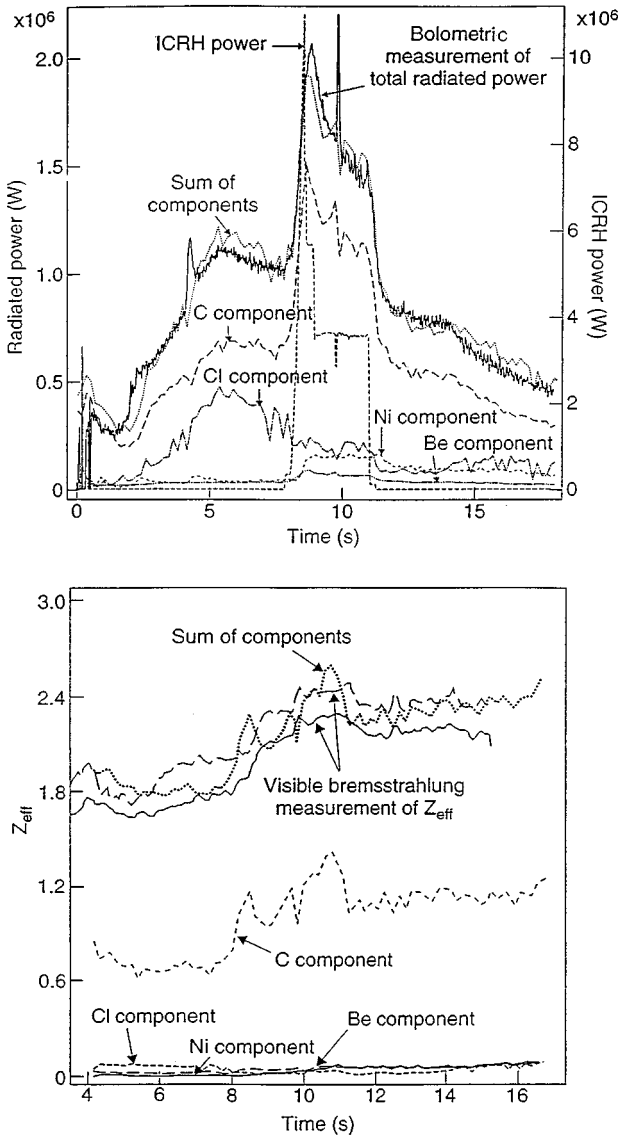

FIG. 4. (upper) Elemental P_{rad} components, the component sum and the total radiated power and (lower) Z_{eff} measurements and components of Z_{eff} together with their sum for pulse No. 19 620. The ICRH power is illustrated (upper), and can be seen to trip after reaching 11 MW.

$Z_{eff}(t,[\text{bremss}])$ is the Z_{eff} determined from visible bremsstrahlung measurements, $C_{eff\text{-}Z}$ a coefficient for a particular element Z and $\overline{z}$ an average charge state of the more central ionization stages of each element. This will equal Z in the case of low Z elements. When dealing with the Z_{eff} it is important to include the contribution of the fuel, here assumed to be a H isotope $(Z=1)$. In summing the radiated power components the contribution of the fuel is usually so small it can be neglected.

III. LINT ANALYSES OF VUV, XUV LINE EMISSION IN LIMITER DISCHARGES

JET limiter discharges, often with auxiliary ICR or other heating, have the demonstrated advantage of pressure profile consistency from one discharge to the next and are exclusively described in this section. Figure 3 illustrates a 3.5 MA deuterium plasma discharge (No. 13 728) with up to 10 MW of ICR heating on the minority $_3$He ions which shows but two main impurities, carbon from the plasma facing components and nickel from the antenna screens. In this case LINT satisfactorily accounts for the elemental contributions to the total power loss and to the global Z_{eff} with estimated errors of $\sim\pm 15\%$. Tracking the most dilute impurities is something of a problem with LINT. However, knowledge that the concentrations of these impurities remain low is of itself valuable and is illustrated by the ICR heated plasma (No. 19 620) in Fig. 4. In this example the Ni emission rises only marginally during ICRH while C impurity and the D fuel account almost exclusively for Z_{eff}.

IV. EXTENSION OF LINT ANALYSES TO THE X-RAY SPECTRUM

The x-ray emission database should also be relevant and amenable to LINT analyses not least because in high tem-

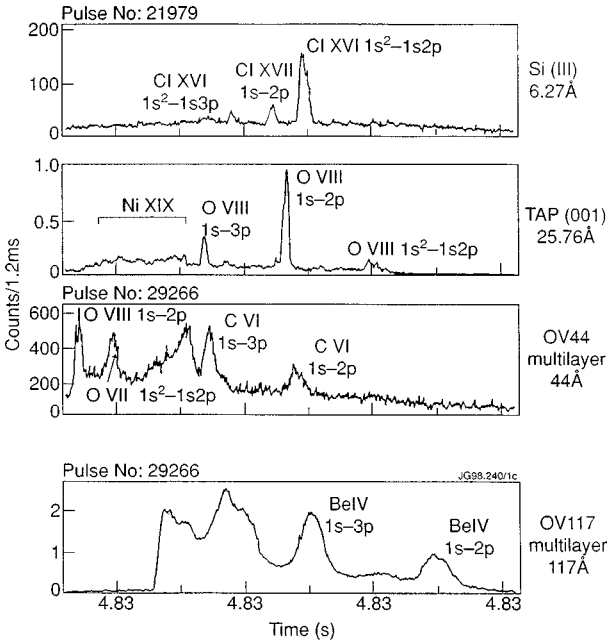

FIG. 5. Spectral surveys of the x-ray emission from JET. The different spectral regions are recorded simultaneously as a function of time using separate diffractors on a reciprocating spindle. In this configuration, the Bragg survey instrument has a modest resolving power ~150, due to the aperture of the beam line.

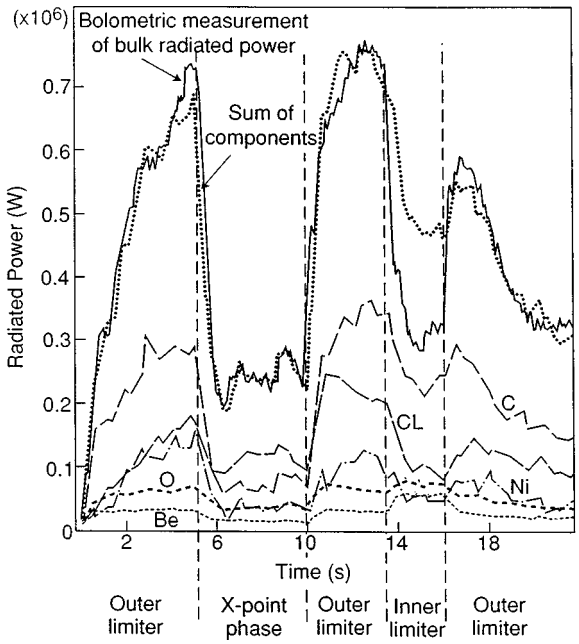

FIG. 6. LINT analyses of reference discharge No. 29 724 using x-ray line intensity data.

perature tokamaks most of the radiation from the bulk plasma lies in the x-ray region where the sensitivity of detectors and spectrometers to absolute photon flux[9] is more readily calculable than is the case in the VUV region. The use of organic crystals and synthetic multilayers has extended[10] the long wavelength limit for Bragg reflection to $\lambda \geqslant 100$ Å, thus overlapping the XUV region. A survey of the x-ray spectrum from JET (No. 29 179, taken at 4.85 s after the start of the current pulse) is shown in Fig. 5. In this survey mode the resolving power of the Bragg spectrometer[10] is limited to about 150 by the aperture of the input optics. Table I includes the main ions and transitions used in this application[11,12] of LINT to the x-ray line emission.

Using these, Fig. 5, and similar Bragg diffraction data, LINT coefficients have been deduced over a number of ''reference'' discharges where, as the magnetic topology or configuration is allowed to vary, the impurity content is assessed throughout the pulse duration ~20 s. The results are shown in Fig. 6. Reassuringly, the sum of the elemental components of $\Sigma P_{\mathrm{RAD}}(Z)$ follows the bolometric signal even as the magnetic configuration is switched into a lower X point at ~5 s from the start of the current pulse. The underlying free–free and free–bound x-ray continuum, $I_{\mathrm{ff+fb}} = n_e^2 Z_{\mathrm{eff}}(C_{\mathrm{ff}} + C_{\mathrm{fb}}) f(T_e)$ is an extremely useful input to the data base, being directly proportional to Z_{eff}. The derivation in JET of Z_{eff} from the x-ray continuum has not yet been done but Fig. 7 shows that the underlying continuum emission recorded by the Bragg spectrometer is measurable[11,12] and is not a spurious signal due to scattered light. Spectrally integrated regions of the x-ray continuum form part of the CATS data base. These soft x-ray ''pinhole'' cameras[13] employ arrays of Si diode detectors with typically a 250-μm-thick Be filter, giving a low energy cutoff of ~2.0 keV. In principle, LINT coefficients could be applied to the absolute continuum intensity to derive the elemental components $Z_{\mathrm{eff}\text{-}Z}$.

TABLE I. X-ray lines used in LINT analyses of JET reference discharges.

$Z(z)$	λ_{ij}	Diffractor
O VIII	Ly-α	TlAP
C VI	Ly-α	OV44
Be IV	Ly-α	OV117
Cl XVI	4.444 (Å)	Si(III)
Ni XXV	9.967 (Å)	TlAP (second order)

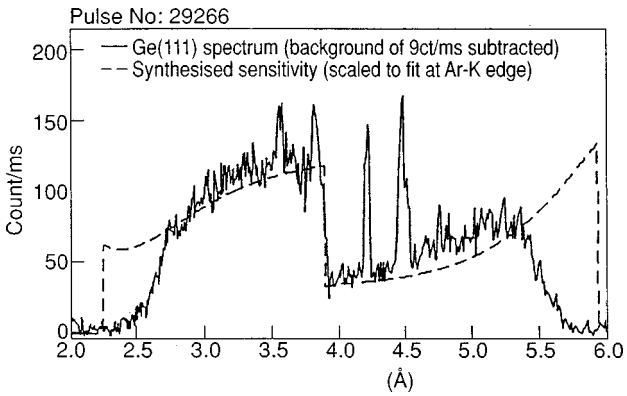

FIG. 7. Ge(111) spectrum of the JET emission using the Bragg survey spectrometer. The resonance lines in the spectrum from Cl XVI and Cl XVII ions are superimposed on the underlying x-ray continuum, the intensity of which is indicated by the step height at 3.87 Å due to absorption in the Ar component in the gas detector.

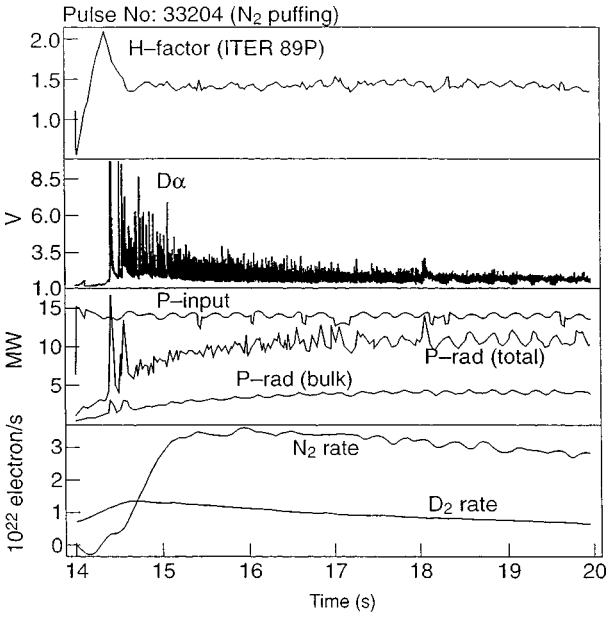

FIG. 8. Diagnostic data pertaining to ELMY H-mode JET discharge No. 33 204 with N_2 gas injection.

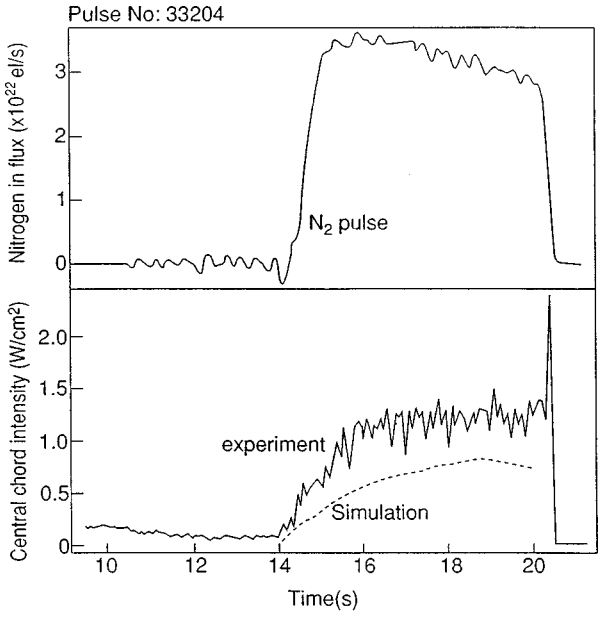

FIG. 9. N_2 pulse (above) injection into JET discharge No. 33 204 showing (below) a comparison of the absolute radiance of an x-ray line, $L\alpha$ (N VII), along a central horizontal chord (experiment) with the results of the SANCO simulation based on transport modeling of nitrogen ions. The code is placed on an absolute basis by normalizing to visible charge exchange measurements of the N^{7+} concentration at a given value of r/a.

V. ELMY H-MODES PLASMAS WITH GAS INJECTION

Experience with the LINT analyses has taught us that empirical fitting of line intensities to P_{RAD} is generally less successful, i.e., has errors much greater than the $\pm 15\%$ accuracy experienced with limiter plasmas, when applied to tokamak plasmas which have local steps in the pressure or radiation profiles. Divertor discharges with edge-radiation cooling, detached plasmas, plasmas with localized edge condensations,[14] or ''MARFE'S,'' enhanced confinement plasmas[15] such as hot-ion H modes or optimized-shear modes come into this category. In the case where the pressure profile is intermittently relaxed due to localized edge modes, ELMs, the situation is favorable to LINT analyses. Such a case is illustrated in Fig. 8 where a pulse of N_2 gas is injected into a diverted JET plasma heated with up to 18 MW of atomic beams. These radiatively cooled discharges are characterized by continuous ''grassy'' ELM activity with an associated, quiescent $H\alpha$ signature (Fig. 8), and an enhanced confinement or ''H factor'' (relative to ITER 89P scaling[16]) of between 1.5 and 2.0. P_{RAD} is about 80% of the input power P_{IN} in these discharges, about one third of which ($\sim$4 MW) radiates from the bulk plasma, while the rest comes from the SOL and divertor region, i.e., between $r/a=1$ and the wall as shown schematically in Fig. 2. Impurity transport calculations are normalized to measurements of the absolute concentrations of N^{7+}, C^{6+} from a charge exchange[17] spectroscopic viewing line intersecting the heating beam at $r/a=0.4$. The resulting radiance simulations of N VII $L\alpha$ along a central chord are less than satisfactory when compared in Fig. 9 to the absolute radiance data from the calibrated Bragg spectrometer. In contrast, Fig. 10, a LINT analysis of the dominant N_2 radiation loss from the bulk plasma predicts to a good accuracy the total confined plasma radiation P_{RAD} measured by bolometry. When the carbon emission is also taken into account using the LINT method, the total elemental power loss agrees with P_{RAD} within an error of $\sim 15\%$.

In limiter discharges it has been shown[3] that the accuracy of fitting LINT data to P_{RAD} and the extent of the data base accumulated over successive time intervals imposes an over constraint on the range of transport parameters which can be allowed in the simulations. Essentially LINT intro-

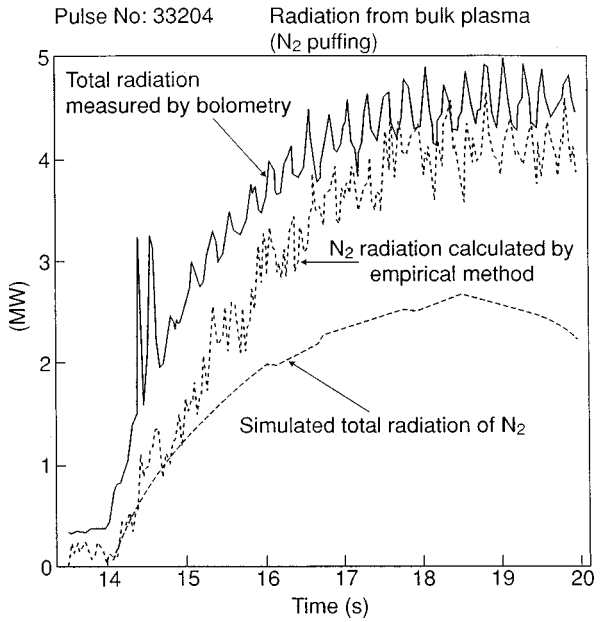

FIG. 10. Comparisons of $P_{\mathrm{RAD\text{-}BOLO}}(t)$ with the empirical LINT analysis of $P_{\mathrm{RAD}\text{-}Z}$, for element N_2 which accounts for 80% of the bulk radiation from JET discharge No. 33 204. The difference $P_{\mathrm{RAD\text{-}BOLO}}(t)-P_{\mathrm{RAD}\text{-}Z}(Z=7)$ can be accounted for by $P_{\mathrm{RAD}\text{-}Z}(Z=6)$. The modulation is due to X-point sweeping. Results using the diffusive ion emission simulation code SANCO are also shown. The code is placed on an absolute basis by referring to the N^{7+} concentration at a given value of r/a.

duces corrections to the detailed modeling of radiation losses in tokamaks. This is the reverse situation from that which is normally assumed, i.e., that sophisticated modeling should lead to a better appreciation of the underlying physics than would an empirical technique like LINT.

VI. SUMMARY

A novel, empirical technique, LINT, has been shown to be a powerful technique for assessing the bulk plasma impurity behavior on a shot-by-shot basis in tokamaks. The method seems to work best, within about 15% error level, for a series of discharges which have a high degree of pressure profile consistency. In some configurations where the method is less satisfactory, e.g., MARFEs, the use of multiple plasma zones, each with their characteristic LINT normalization factors may be an answer. For tokamaks with very long pulse durations, e.g., TORE SUPRA or the ITER proposal, transport simulations and LINT coefficients could be adjusted near the beginning of the current pulse and the empirical technique used thereafter to track impurities with some confidence provided that the electron pressure profile remains consistent.

ACKNOWLEDGMENTS

This work forms part of a Task Agreement between JET and UKAEA-Fusion and is funded by the U.K. Department of Trade and Industry and EURATOM.

[1] L. Lauro-Taroni *et al.*, Proceedings of the 21st EPS Conference on Controlled Fusion and Plasma Physics, Montpellier (1994), Vol. 1, p. 102.
[2] H. P. Summers and M. von Hellermann, in *Atomic and Plasma-Material Interaction Processes in Controlled Thermonuclear Fusion*, edited by R. K. Janev and H. W. Drawin (Elsevier Science, New York, 1993), pp. 87–117.
[3] K. D. Lawson *et al.*, Phys. Rev. (submitted).
[4] R. J. Fonck *et al.*, Appl. Opt. **21**, 2115 (1982).
[5] N. C. Hawkes *et al.*, *Proceedings Tenth International Coll. UV and X-Ray Spectroscopy of Astrophysical and Laboratory Plasmas, Berkeley*, edited by E. H. Silver and S. M. Kahn (Cambridge University Press, Cambridge, 1992), p. 324.
[6] J. L. Schwob *et al.*, Rev. Sci. Instrum. **58**, 1601 (1987).
[7] K. F. Mast *et al.*, Rev. Sci. Instrum. **56**, 969 (1985).
[8] P. D. Morgan and J. J. O'Rourke, Proceedings 14th EPS Conference on Controlled Fusion and Plasma Physics, Madrid (1987), Vol. 3, p. 1240.
[9] N. J. Peacock *et al.*, Rev. Sci. Instrum. **66**, 1175 (1995).
[10] R. Barnsley *et al.*, *UV and X-Ray Spectroscopy of Laboratory and Astrophysical Plasmas* (Cambridge University Press, Cambridge, 1993), p. 513.
[11] R. Barnsley *et al.*, *Diagnostics for Experimental Thermonuclear Fusion Reactors*, edited by P. E. Stott, G. Gorini, and E. Sindoni (Plenum, New York, 1996), pp. 353–364.
[12] R. Barnsley *et al.* Workshop on Diagnostics for Experimental Thermonuclear Fusion Reactors, JET Preprint No. P(97)36, 1997.
[13] A. W. Edwards *et al.*, Rev. Sci. Instrum. **57**, 2142 (1986).
[14] B. Lipschultz, J. Nucl. Mater. **145–147**, 15 (1987).
[15] G. T. A. Huysmans, JET Preprint No. JET-P(98) 09, 1998.
[16] P. N. Yushmanov *et al.*, Nucl. Fusion **30**, 1999 (1990).
[17] M. von Hellermann and H. P. Summers, in *Atomic and Plasma-Material Interaction Processes in Controlled Thermonuclear Fusion*, edited by R. K. Janev and H. W. Drawin (Elsevier Science, New York, 1993), pp. 135–163.